Naftali (Tuli) Herscovici
Spike Technologies, Inc.
1 Chestnut St.
Nashua, NH 03060 USA
+1 (603) 594-8856
+1 (603) 577-9647 (Fax)
naftali.Herscovici@ieee.org (e-mail)

Christos Christodoulou
Department of Electrical and
Computer Engineering
University of New Mexico
Albuquerque, NM 87131-1356 USA
+1 (505) 277-6580
+1 (505) 277-1439 (Fax)
christos@eece.unm.edu (e-mail)

Smart Antennas in Wireless Communications: Base-Station Diversity and Handset Beamforming

Carl B. Dietrich, Jr., Warren L. Stutzman, Byung-Ki Kim, and Kai Dietze

Virginia Tech Antenna Group, Electrical and Computer Engineering Department, Blacksburg, VA 24061-0111 USA
http://www.ee.vt.edu/antenna

Keywords: Land mobile radio cellular systems; land mobile radio equipment; land mobile radio diversity systems; array signal processing; land mobile radio cellular handsets; smart antennas

1. Introduction

As wireless-communication systems evolve, service quality and capacity are of primary importance. To ensure reliable communication over a mobile-radio channel, a system must overcome multipath fading, polarization mismatch, and interference. The trend towards low-power handheld transceivers increases all of these challenges. Even as more spectrum is allocated, demand for higher-data-rate services and steadily increasing numbers of users will motivate wireless service providers to seek ways of increasing system capacity.

Antenna arrays can improve reliability and capacity in three ways. First, diversity-combining techniques combine the signals from multiple antennas in a way that mitigates multipath fading. Second, adaptive beamforming–using antenna arrays–provides capacity improvement through interference reduction, and also mitigates multipath fading. In cellular systems, the use of adaptive arrays is an alternative to the expensive approach of cell splitting, which increases capacity by increasing the number of base-station sites. Adaptive arrays cancel or coherently combine multipath components of the desired signal, and null interfering signals that have different directions of arrival from the desired signal. A third category of systems uses switched fixed beams to achieve coarser pattern control than adaptive arrays, but to still provide some capacity improvement. Two or more of the fixed beams can be used for diversity reception. Adaptive and switched-beam antenna systems are popularly referred to as "smart antennas," because of the dynamic system intelligence required for their operation. Most arrays that have been considered for such applications are located at the base station, but now they are also under consideration for handheld terminals.

Some researchers have proposed diversity combining at the terminals (i.e., the handheld radios), and have shown that significant performance gains can be achieved. The use of adaptive antennas on handheld radios is a new area of research. In 1988, Vaughan [1] concluded that with then-current technology, adaptive beamforming was feasible for units moving at pedestrian speeds, but not for high-speed mobile units. Lian [2] suggested the use of handheld arrays in mobile satellite systems. In 1999, Braun et al. [3] reported on indoor experiments in which data were recorded using a stationary narrowband transmitter and a two-element handheld receiving antenna array. In [3], data recorded over different paths were treated as desired and interfering signals, and the uncorrupted desired signal–unavailable in practice–was used as a reference signal for optimum beamforming. While these experiments do not correspond to actual operating conditions, interference rejection of 24 dB in the single-interferer case and 16 dB in the two-interferer case was reported in two handset configurations.

Multi-polarized adaptive arrays, sometimes called polarization-sensitive adaptive arrays, are used to match the polarization of a desired signal or to null an interferer having the same direction of arrival as the desired signal, if the two signals have different polarization states. If base stations or mobile units in a peer-to-peer system can match the polarization states of hand-held transceivers, link quality and reliability will be enhanced, and power consumption in the handheld units will be reduced, increasing battery life. It is possible that a 100% or greater increase in system capacity can be achieved through a combination of spatial and polarization reuse. Because they offer large, untapped potential performance gains, multi-polarized adaptive arrays are being studied extensively to determine what performance improvements are feasible. Currently, however, little is known about the performance of multi-polarized adaptive arrays in mobile-communication systems.

Multi-polarized arrays have been considered as a means of rejecting jammers in military applications [4-6]. The potential of multi-polarized arrays for interference rejection in wireless-communication systems has been investigated in recent years for base stations [6-9]. This research considers only free-space propagation, and indicates that 20 to 35 dB of interference rejection is possible, if interfering and desired signals differ in either polarization state or angle of arrival. However, neither measurements nor simulations have been reported that show the performance of multi-polarized adaptive arrays in typical mobile multipath channels.

In this paper, we review diversity and smart-antenna research applied to both base stations and terminals. To illustrate performance gains possible, the paper describes research being conducted by the Smart Antenna Group at Virginia Tech, in both smart base stations and smart handheld terminals.

2. Diversity Combining [10, 11]

Antenna arrays provide signals that can be combined using diversity techniques to improve performance in fading channels. Figure 1 depicts the block diagrams of three diversity-combining techniques. Selection diversity, shown in Figure 1a, is the simplest of these methods. From a collection of M antennas, the branch with the largest signal-to-noise ratio at any time is selected and connected to the receiver. As one would expect, the larger the value of M, the higher the probability of having a larger signal-to-noise ratio (SNR) at the output. Maximal-ratio combining takes better advantage of all the diversity branches in the system. Figure 1b shows this configuration where all M branches are weighted with their respective instantaneous signal-voltage-to-noise ratios. The branches are then co-phased prior to summing, in order to ensure that all branches are added in phase for maximum diversity gain. The summed signals are then used as the received signal. Maximal-ratio combining has advantages over selection combining, but is more complicated; proper care has to be taken in order to ensure that signals are co-phased correctly, and gain coefficients have to be constantly updated. A variation of maximal-ratio combining is equal-gain combining (see Figure 1c). In this scheme, the gains of the branches are all set to the same value, and are not changed thereafter. As with the previous case, the output is a co-phased sum of all the branches.

3. Smart Antennas

Smart antennas vary from simple switched-beam configurations to fully adaptive arrays. Switched-beam arrays use beamforming techniques that yield multiple, fixed, simultaneously available beams. The beams can have high gain and low sidelobes, or controlled beamwidth. Adaptive-beamforming techniques dynamically adjust the array pattern to optimize some characteristic of the received signal. Beam-scanning systems are also possible, in which a single main beam is steered, and the direction is varied either continuously or in small discrete steps.

Antenna arrays using adaptive-beamforming techniques can reject interfering signals having a direction of arrival different from that of a desired signal. Multi-polarized adaptive arrays can also reject interfering signals having polarization states that differ from the desired signal, even if the signals have the same direction of arrival. These capabilities are exploited to improve the capacity of wireless-communication systems.

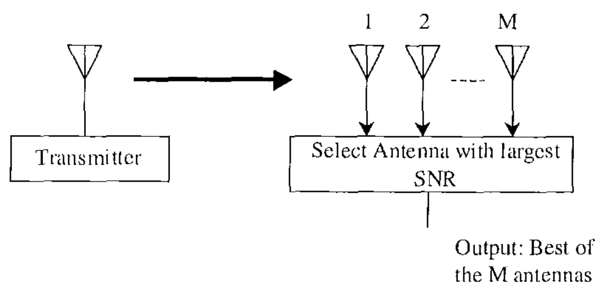

Figure 1a. Diversity combing techniques: selection diversity [11].

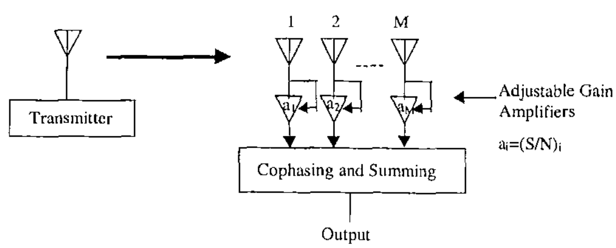

Figure 1b. Diversity combing techniques: maximal-ratio combining [11].

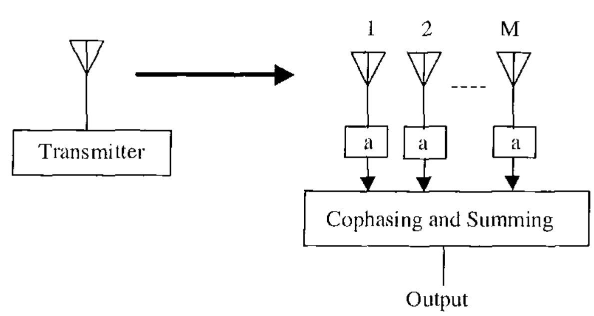

Figure 1c. Diversity combing techniques: equal-gain combining [11].

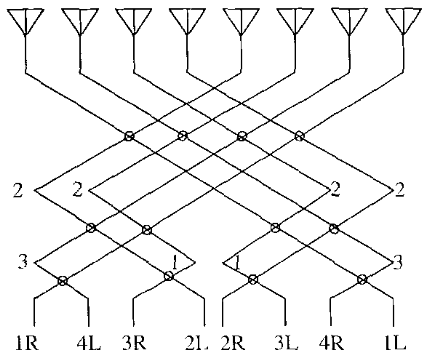

Figure 2. An 8×8 Butler matrix feeding an eight-element array ($n = 3$). The circles are 90° hybrids, and the numbers are phase shifts in units of $\pi/8$ [14].

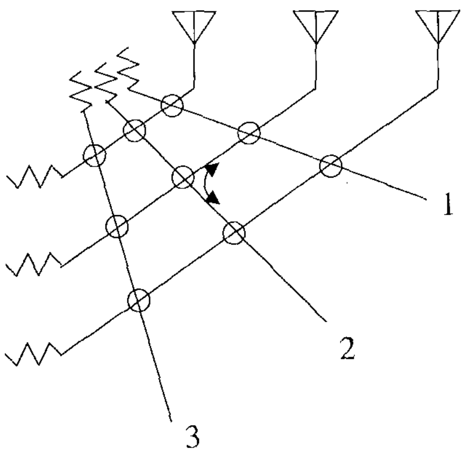

Figure 3. A Blass matrix. The circles are directional couplers.

Smart antennas are being deployed in wireless-communication systems. Smart antennas can increase the coverage and capacity of a system using several approaches, including range extension, interference reduction and rejection, spatial-division multiple access (SDMA), CDMA/SDMA or pseudo-SDMA, and multipath mitigation through diversity combining. These are further discussed in [12] and [13]. Sector shaping is also possible, using switched-beam base-station antennas. Arrays can also be used to improve the performance of mobile or handheld units in both cellular and peer-to-peer systems, with system-level benefits.

3.1 Beamforming Techniques for Switched-Beam Arrays

Some array applications require several fixed beams that cover an angular sector. Several beamforming techniques exist that provide these fixed beams. Two common realizations make use of a Butler Matrix or a Blass Matrix, which are discussed below.

The Butler matrix [14] is a beamforming network that uses a combination of 90° hybrids and phase shifters. An 8×8 Butler matrix is shown in Figure 2 [14]. The Butler matrix performs a spatial fast Fourier transform, and provides 2^n orthogonal beams. These beams are linearly independent combinations of the array-element patterns.

When used with a linear array, the Butler matrix produces beams that overlap at about 3.9 dB below the beam maxima. A Butler-matrix-fed array can cover a sector of up to 360°, depending on element patterns and spacing. Each beam can be used by a dedicated transmitter and/or receiver; or a single transmitter and/or receiver can be used, and the appropriate beam can be selected using an RF switch. A Butler matrix can also be used to steer the beam of a circular array, by exciting the Butler-matrix beam ports with some additional amplitude and phase weighting [15].

The Blass matrix [16] uses transmission lines and directional couplers to form beams by means of time delays, and thus is suitable for broadband operation. Figure 3 shows an example for a three-element array, but a Blass matrix can be designed for use with any number of elements. Port 2 provides equal delays to all elements, resulting in a broadside beam. The other two ports provide progressive time delays between elements, and produce beams that are off-broadside. The Blass matrix is lossy because of the resistive terminations. In one recent application [17], a three-element array, fed by a Blass matrix, was tested for use in an antenna-pattern diversity system for a handheld radio. The matrix was optimized to obtain nearly orthogonal beams.

Fixed beams can also be formed using a Wullenweber array [15], or using lens antennas--such as the Luneberg lens or Rotman lens--with multiple feeds. Lenses focus energy radiated by feed antennas that are less directive. Lenses can be made from dielectric materials or implemented as space-fed arrays. Multi-beam arrays can be used to feed reflector antennas, as well.

3.2 Adaptive Antennas

Adaptive antennas are dynamically controlled to direct beams toward desired users by element-excitation adjustments, rather than by performing just a switching operation.

3.2.1 Optimum Beamforming

Complex weights for each element of an array can be calculated to optimize some property of the received signal. This does not always result in an array pattern with a beam maximum in the direction of the desired signal, but does yield the optimal array-output signal in terms of the minimum-mean-squared error (MMSE), or the maximum signal-to-interference-plus-noise ratio (SINR). Most often, this is accomplished by forming nulls in the directions of interfering signals. Adaptive beamforming is an iterative approximation of optimum beamforming.

A general array, with adjustable element weights, is shown in block-diagram form in Figure 4. The output of the array, $y(t)$, is the weighted sum of the received signals, $s_i(t)$, at the array elements having patterns $g_m(\theta,\phi)$ (the patterns include gain) and the thermal noise, $n(t)$, from receivers connected to each element. In the case shown, $s_1(t)$ is the desired signal, and the remaining L signals are considered to be interferers. In general, the signals

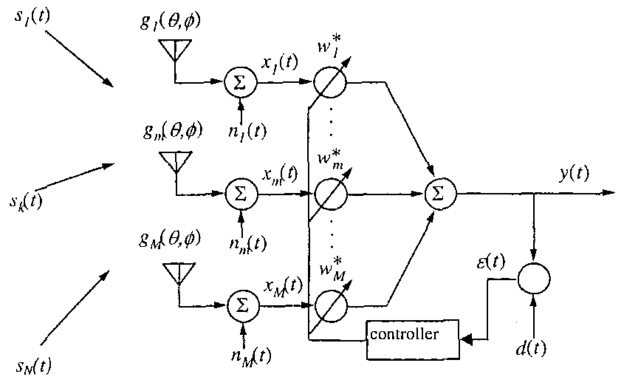

Figure 4. An adaptive antenna array.

$s_i(t)$ include multipath components. In an adaptive system, the weight vector, w, comprising weights w_m, is iteratively determined, based on the complex scalar-array output, $y(t)$; a reference signal, $d(t)$, which approximates the desired signal; and previous weights. In Figure 4 and the following discussion, the symbol * denotes the complex conjugate. The reference signal is assumed to be identical to the desired signal. In practice, this can be achieved or approximated using a training or synchronization sequence or a CDMA spreading code, which is known at the receiver.

The array output is given by

$$y(t) = w^H x(t), \qquad (1)$$

where w^H denotes the complex-conjugate transpose of the $M \times 1$ weight vector w, and $x(t)$ is an $M \times 1$ vector of the received signals and noise. The optimum weights minimize the mean-squared error, $\varepsilon(t)$, between the array output and the reference signal. A desired signal, $s_1(t)$, L interfering signals, and additive white Gaussian noise are considered in the derivation. Rather than the usual implicit assumption of isotropic elements, general directional element patterns are considered. The element patterns need not be the same for all elements.

3.2.2 Optimum Weights and Adaptive Algorithms

To optimize the element weights, we seek to minimize the mean-squared error between the array output and the reference signal, $d(t)$. The derivation proceeds as for the case of omnidirectional elements, and the solution for the optimum weights is

$$w_{opt} = R_{xx}^{-1} r_{xd}, \qquad (2)$$

where $R_{xx} = x(t)x^H(t)$ is the signal covariance matrix, and $r_{xd} = d^*(t)x(t)$. This is identical to the expression for the optimum weights for an array with isotropic elements (see [18]). In this case, however, R_{xx}, r_{xd}, and, hence, w_{opt} are functions of the angles of arrival of the $L+1$ signals, and of the element patterns.

Adaptive-beamforming algorithms iteratively approximate the optimum weights. Adaptive beamforming began with the work of Howells [19] and Applebaum [20]. Several newer beamforming algorithms are described in [18].

The next two sections describe experimental investigations of diversity reception at cellular base stations, and adaptive beamforming using small portable and handheld arrays.

4. Base-Station Diversity Experiments

Diversity techniques are used at the base station to overcome multipath fading. Although space diversity is the most common form of antenna diversity, it is the least attractive, because it requires a second antenna subsystem. A separate diversity antenna requires space and cable runs, and significantly increases installation and maintenance costs. The remaining diversity choices are angle and polarization diversity. Recent interest has focused on polarization diversity that uses a single, dual-polarized antenna in

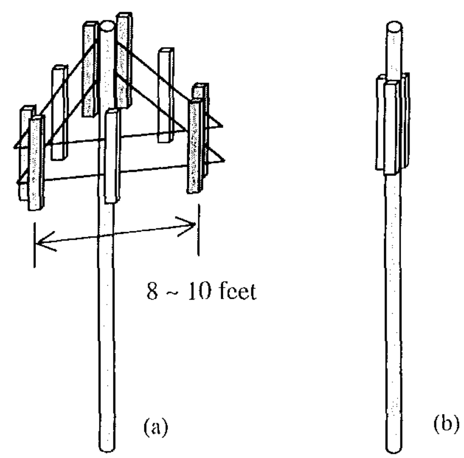

Figure 5. A typical three-sector configuration: (a) Space-diversity installation; (b) Polarization-diversity installation.

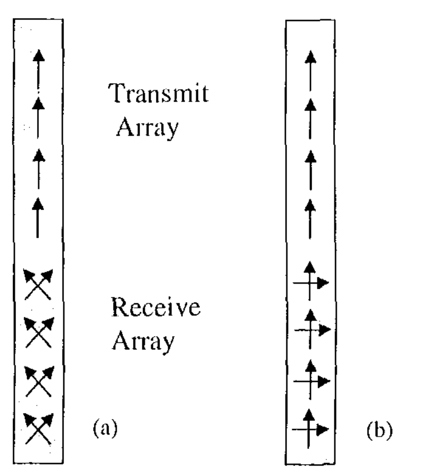

Figure 6. Two antenna configurations for polarization diversity: (a) Slant ±45° receive; (b) V/H receive.

Table 1. The smart base-station receiver channels.

Channel Number	1	2	3	4	5	6	7	8
Symbol	S1	P1	P2	A1	A2	A3	A4	S2

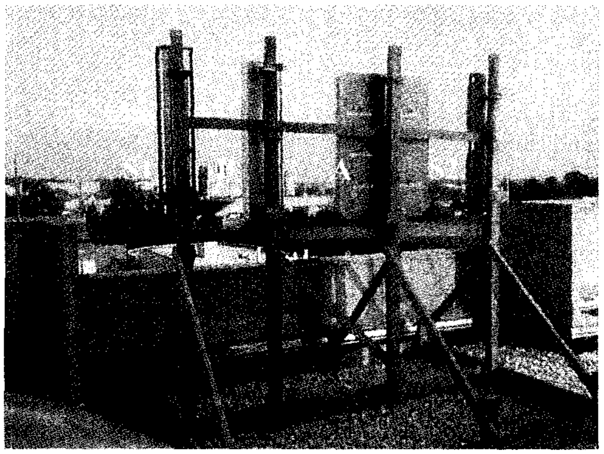

Figure 7a. The smart base-station antenna hardware at Virginia Tech: the antenna assembly on the roof of a six-story-high building. From left to right are the 95° sector (S1), dual-polarized (P1, P2), 4 × 30° narrow beam (A1, A2, A3, A4), and 95° sector antennas (S2).

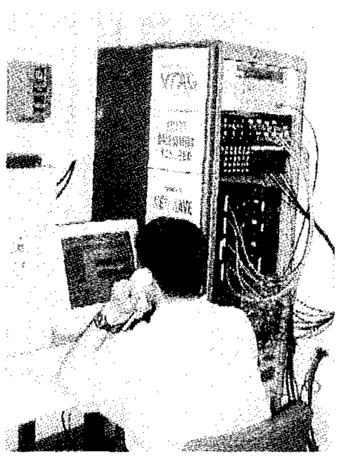

Figure 7b. The smart base-station antenna hardware at Virginia Tech: the receiver equipment.

place of two space-diversity antennas [25]. Angle diversity with switched-beam antennas is also effective in urban environments [26], but its performance with indoor mobile users has not yet been reported. No direct, simultaneous performance comparisons of space, polarization, and angle diversity have been reported.

4.1. Overview of Base-Station Diversity Systems

A typical sector base station with space diversity consists of two spatially separated receive antennas and one transmit antenna per sector. In the typical three-sector configuration, a total of nine antennas is required, as shown in Figure 5a. However, polarization diversity performs the same function with three antennas, as shown in Figure 5b, using one of the antenna configurations in Figure 6. Several papers have reported that the slant ± 45° configuration is slightly better (~1 dB) than the V/H configuration in polarization diversity, due to the balanced mean powers between channels [25-31]. Also, it is known that a polarization-diversity system is more effective when the orientation of the mobile-unit antenna is slanted.

Angle diversity is implemented using a switched-beam antenna in cellular-radio and digital personal-communication systems. Although fully adaptive antennas are more flexible, a switched-beam antenna is relatively easy to implement, and is cost effective. This system also can be used to synthesize sectors with a balanced traffic load to increase channel capacity [32]. Perini and Holloway [33] reported that in dense urban areas, angle diversity is just as effective as conventional spatial diversity, and provides about 8 dB of diversity gain at the 99% reliability level.

4.2. Smart Base-Station Testbed at Virginia Tech

The smart base-station hardware at Virginia Tech consists of a mobile transmitter, operating at 842 MHz in the cellular band, and a rooftop base station, operating as a receiver. The receiver has eight channels connected to three types of base-station antennas, as listed in Table 1 along with assigned channel names. In Table 1, S stands for antenna for "space diversity," P stands for "polarization diversity," and A stands for "angle diversity." S1 is used as a reference channel through the measurement and calibration process.

Figure 7 shows the configuration of the base-station testbed, as installed on the roof of a six-story building that is 30 m above the ground. The order of the antennas, viewed from behind the

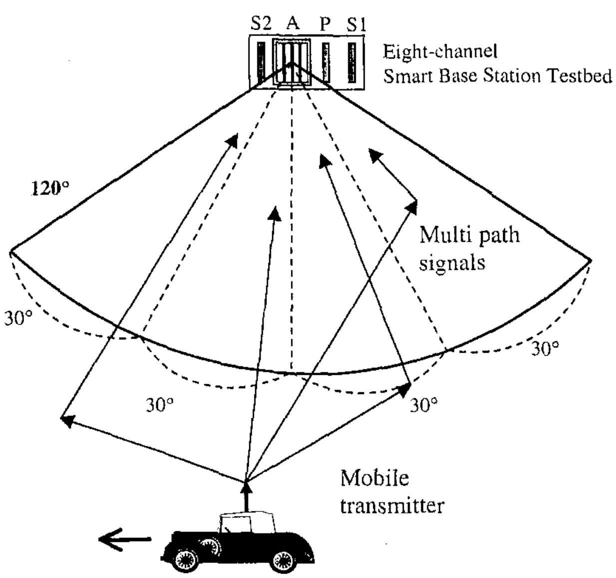

Figure 8. An eight-channel smart base-station testbed for space, polarization, and angle-diversity comparisons in a multipath environment.

supporting structure as shown in Figure 7, from left to right are the 95° sector (S1), dual-polarized (P1, P2), 4 × 30° narrow beam (A1, A2, A3, A4), and 95° sector antennas (S2). The height of the supporting structure is 10 ft, and the separation between space diversity antennas is about 10 ft (8.5 wavelengths at 842 MHz).

The 4 × 30° panel antenna (A1, A2, A3, and A4) covers 120°, as shown Figure 8; the sector antennas (S1, S2) cover 95°; and the ± 45° slanted dual polarized antenna (P1, P2) covers 90°. All have a vertical beamwidth of about 15°. The 90° and 95° azimuth beamwidth of the dual-polarized and sector antennas can be considered to be identical, for all practical purposes. The two sector antennas (S1, S2) are used for space diversity. The 4 × 30° panel antenna (A1 to A4) is used for angle diversity, and the dual-polarized antenna is for polarization diversity. In order to obtain high diversity gain, low correlation and power balance are important. Space diversity requires wide separation between two antennas to achieve a low correlation between the signals. The ± 45° slanted dual-polarized antenna is known to have highly balanced power.

The mobile unit, moving at a speed of about 1~2 m/s, transmits a continuous-wave signal at 842.07 MHz. The eight RF signals received at the base station are down-converted to a 1.2 kHz IF, using RF mixers with the same local oscillator that maintains the relative amplitude and phase information between channels. The IF signals are recorded with a 16-bit A/D converter, running at a sampling rate of 6.25 kHz per channel, and are then post-processed in non-real time.

Measurements are performed for various mobile-transmitter unit locations, using a half-wavelength dipole antenna in three orientations: (a) vertical (V), (b) horizontal and orthogonal to the direction of movement (H+), (c) horizontal and parallel to the direction of movement (H||). The operator of the mobile unit is equipped with a cellular phone, for voice communication with the operator at the base station. All measurements are performed along straight routes. Measured runs are performed over distances of 60 to 130 m for the outdoor environments, and 35 to 50 m for the indoor environments. The average velocity of the mobile unit is calculated using the measured distance and time for every run. The distance between the mobile unit and the base station is measured using both a GPS receiver and electronic maps in *AutoCAD* format; the distance ranges from 150 m to 5 km.

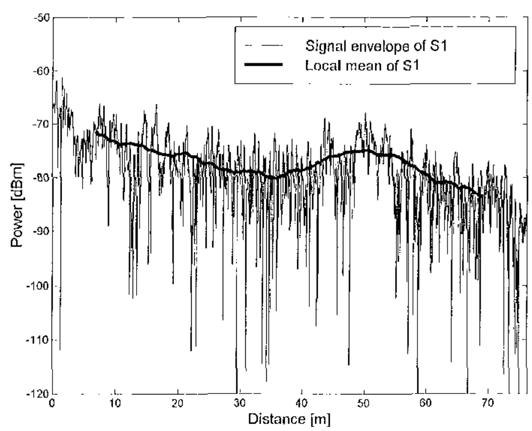

Figure 9a. The signal envelope and cumulative distribution functions (CDFs) for three kinds of diversity under identical conditions: The measured signal envelope of one channel with the estimated local mean.

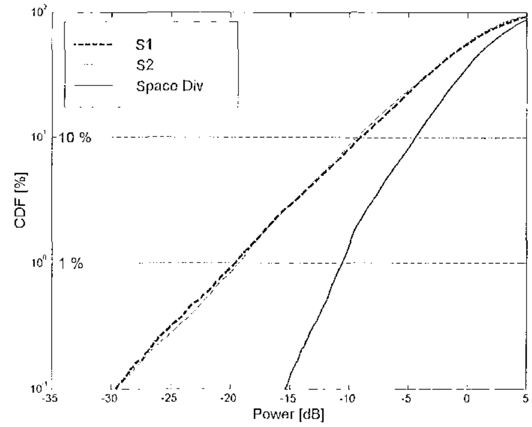

Figure 9b. The signal envelope and cumulative distribution functions (CDFs) for three kinds of diversity under identical conditions: The CDF for space diversity.

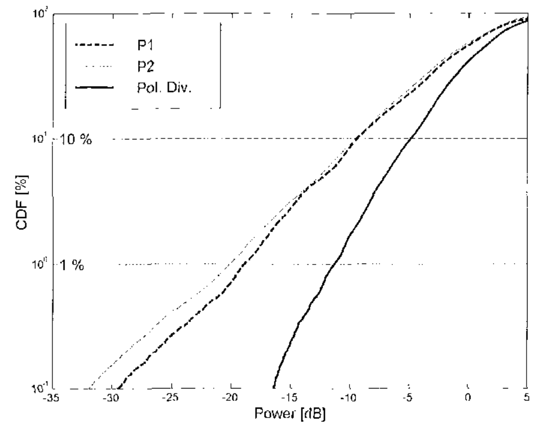

Figure 9c. The signal envelope and cumulative distribution functions (CDFs) for three kinds of diversity under identical conditions: The CDF for polarization diversity.

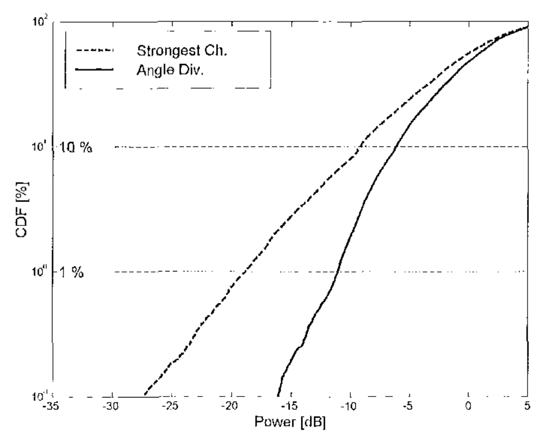

Figure 9d. The signal envelope and cumulative distribution functions (CDFs) for three kinds of diversity under identical conditions: The CDF for angle diversity.

Table 2. The measured diversity gain (in dB).

		At 665 m			At 935 m			At 2,670 m		
Pol.	CDF	S	P	A	S	P	A	S	P	A
V	10 %	5.15	4.45	3.61	4.83	4.61	3.07	5.52	4.65	1.50
	1 %	8.91	8.42	8.72	8.86	8.19	7.79	10.24	8.47	6.33
H+	10 %	5.23	3.82	2.54	5.06	5.19	2.18	5.52	5.12	0.86
	1 %	9.70	6.59	8.26	9.79	10.12	6.06	10.72	9.74	4.62
H||	10 %	5.65	5.13	3.61	5.08	4.50	2.96	5.65	5.07	1.72
	1 %	10.88	8.91	8.97	9.34	8.47	7.59	9.99	9.41	6.63

4.3 Estimation of Local Mean

The instantaneous fading-signal envelope, $r(t)$, received at the base-station antenna, can be separated into two terms [34, 35]: $m(t)$ represents the long-term signal fading (or local mean), and $f(t)$ represents the short-term (Rayleigh) signal fading. The relationship among these three parameters is expressed by

$$r(t) = m(t)f(t). \tag{3}$$

The position, x, is related to time, t, through the constant speed of the transmitter, v:

$$x = vt. \tag{4}$$

Then, $r(t)$ can be represented in the spatial domain as follows:

$$r(x) = m(x)f(x). \tag{5}$$

The estimate of the local mean, $\hat{m}(x)$, at a spot x, averaged over a window of length $2L$, can be obtained from

$$\hat{m}(x) = \frac{1}{2L}d\int_{x-L}^{x+L} r(y)dy. \tag{6}$$

A good estimate of the local mean in Rayleigh and Ricean fading channels is obtained for $2L = 40\lambda$ and a number of samples over $2L$, $N = 36$. The window length and number of samples are based on a 90% confidence interval and less than 1 dB of error in estimating the local mean [35]. Figure 9a shows the measured signal envelope and its estimated local mean of S1 over a measurement distance of 250 ft (76 m), when the orientation of the mobile-unit antenna was vertical (V). It should be noted that the differences of the local means between two different points could be more than 10 dB, even in the same measurement run. Therefore, the effect of long-term fading was properly removed to avoid biasing the diversity statistics.

4.4 Initial Measurement Results and Analysis

An initial measurement campaign was conducted in 1999, and data were collected and processed for various diversity-combining techniques. Here, we present some sample results for selection combining. Figures 9b-d show the cumulative-distribution functions (CDFs) for selection combining, while the orientation of the mobile-unit antenna was vertical, at a distance of 935 m. Several measurements at various distances with three orientations of mobile-unit antenna were performed. Table 2 summarizes the measurement results performed at three example locations in non-line-of-sight urban environments. The results measured at a distance of 665 m showed that the diversity gains for the three diversity schemes were close to each other at the 1% level of the CDF, regardless of the orientations of the mobile-unit antenna. Although polarization-diversity gains were close to those for the other kinds of diversity, the performance of polarization diversity was superior when the mobile-unit antenna was horizontal, and was worse with vertical orientation, due to the polarization match. At a distance of 935 m, the space diversity-gain was slightly better than that for the other kinds of diversity, regardless of the orientations of the mobile-unit antenna. At a distance of 2670 m, the space-diversity gain was slightly better than the polarization-diversity gains, and it was several dB better than the angle-diversity gain, regardless of the orientations of the mobile-unit antenna. More than 180 sets of measurements have been performed in over 60 locations. The measurement campaign is still in progress.

5. Handheld Adaptive-Array Experiments

The popularity of the wireless-communication bands has created a condition where systems are often limited by interference. Handheld radios with adaptive antennas can reject interference, and can thus improve communication-link quality and increase system capacity. However, as stated in the introduction, little research in this area has been reported for commercial communications.

The Smart Antenna Group at Virginia Tech has performed an extensive investigation of adaptive beamforming, using compact antenna arrays on a handheld-radio platform. The investigation used small, four-element antenna arrays, mounted on a receiver that could be carried like a mobile phone. This investigation showed that a high degree of interference rejection is possible, indicating that–in a system using handheld radios equipped with adaptive arrays–more than one user can share a frequency channel during the same time slot. This can be done through a spatial-division multiple access (SDMA) scheme, or through a combination of SDMA and code-division multiple access (CDMA). This capacity improvement would allow a commercial mobile-communication system to support more users than a conventional system using the same limited frequency spectrum, resulting in increased revenues. The interference-rejection capability of handheld adaptive arrays also provides protection against jamming in military scenarios.

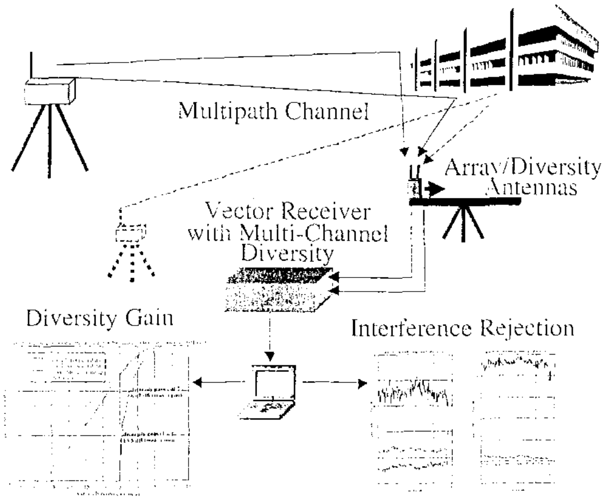

Figure 10. An overview of the Handheld Antenna Array Testbed (HAAT).

5.1 Experiment Description

The adaptive-beamforming measurement campaign has so far produced over 250 experiments in rural, suburban, and urban channels with two mutually interfering transmitters. The performance of single-polarized and multi-polarized four-element compact arrays was measured in outdoor peer-to-peer (distances of 25-50 m, line-of-sight and non-line-of-sight) and microcellular (distances of up to 0.6 km, mostly non-line-of-sight) scenarios. Figure 10 shows the testbed system in a typical experimental scenario. In each measurement, two fixed transmitters transmitted approximately equal-level continuous-wave (CW) signals, offset by 1 kHz, at approximately 2.05 GHz. In some experiments, the receiver was alternately connected to five small four-element array configurations, and was moved along a 2.8 m track to provide consistent results. In other measurements, an operator carried the receiver and antenna array next to his head, to represent a realistic operational scenario. A direct-conversion four-channel receiver that mixed the received signals down to baseband was used. The data were recorded on two portable stereo digital audio tape recorders at 32,000 samples per second per channel, 16 bits per sample. A pulse was recorded at the beginning and end of each measurement to align the data for processing.

5.2 Data Processing

The data were processed on a computer, using a multi-target least-squares constant-modulus algorithm (MT LSCMA). The least-squares constant-modulus algorithm (LSCMA) is a blind adaptive-beamforming algorithm: that is, it does not require precise knowledge of the desired signal, but uses knowledge of the constant-modulus property, common to many waveforms. The weights were calculated using a direct matrix inversion, as follows:

$$w = R_{xx}^{-1} r_{xd}\,, \tag{7}$$

where R_{xx} and r_{xd} are as described in Section 3.2.2, but a constant-modulus estimate of the desired signal, given by $d = \frac{y}{|y|}$, was used.

The Multi-target LSCMA, or MT LSCMA, uses a Graham-Schmidt orthogonalization to produce two or more orthogonal sets of weights. Using purely spatial processing, a multi-target algorithm can separate a number of signals equal to the number of array elements. Soft orthogonalization [23] or hard orthogonalization [24] can be used. Hard orthogonalization is described here. Initially, for an N-element array, N orthogonal weight vectors are used. Each weight vector is updated independently, using the LSCMA as in Equation (7). All but the first weight vector are periodically reinitialized, as follows, to prevent more than one weight vector from converging to the same value:

$$w^k = w^k - \sum_{i=1}^{k-1} \frac{w^{i^H} R_{xx} w^k}{w^{i^H} R_{xx} w^i} w^i\,, \quad k = 2,3,\ldots,M\,. \tag{8}$$

In the experiments described here, an MT LSCMA beamformer was used to calculate element weights for each block of 64 to 320 samples of measured data. The reference signal for the matrix inversion was obtained by normalizing the complex beamformer output to a constant magnitude. The algorithm adaptively calculated and updated two weight vectors, one to optimize reception of each signal. Two iterations of the algorithm were run on each block, and each updated weight vector was applied to the data used to calculate that weight vector. A hard orthogonalization was performed for each block so the two weight vectors did not converge to the same solution. Sometimes, the desired signal switched from one MT LSCMA beamformer output to the other. While knowledge of the signals was not used in the beamforming, the two output signals were interchanged as necessary–using the signal frequency as a criterion–to keep the signal from a given transmitter on the same output port throughout each measurement.

The processing software calculated the signal-to-interference-plus-noise ratio (SINR) and the signal-to-noise ratio (SNR) before and after beamforming for each signal and for each channel. An FFT was performed on each block of data samples. The signal power in a 100 Hz bandwidth, about each of the two received baseband signals (near 4 and 5 kHz, respectively), and the noise power in 100 Hz centered on 7 kHz, were measured. The improvement in SINR at a given cumulative probability level after beamforming is denoted by ΔSINR. The theoretical mean output SNR of an ideal maximal-ratio diversity combiner, in the absence of interference, provided an upper-bound estimate of the mean SINR after beamforming in the presence of interference. This estimate was calculated by summing the mean SNRs of the four channels.

5.3 Experimental Results

A typical experimental scenario is shown in Figure 11. This site is classified as suburban, line-of-sight. The controlled experiments with a receiver that was stationary, or moving at a uniform speed on a linear positioner, showed that the mean SINR for the desired signal could be improved from about 0 dB before beamforming to 30 to 40 dB after MT-LSCMA beamforming. Figure 12 shows the mean SINR results for measurements at the site in Figure 11. Similar improvements in SINR were seen at cumula-

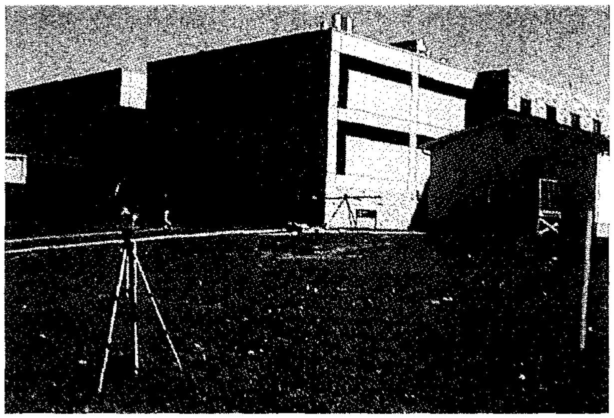

Figure 11. A suburban line-of-sight channel on the Virginia Tech campus: A view with one transmitter in the foreground, looking toward the receiver (the other transmitter is to the right of the picture).

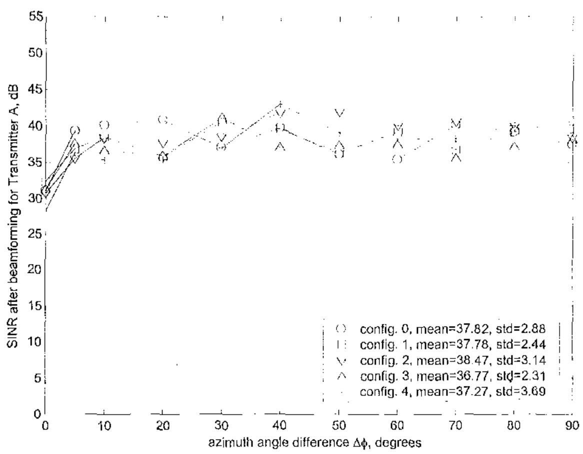

Figure 12. The results of interference-rejection measurements in the suburban line-of-sight environment shown in Figure 11: The mean SINR after adaptive beamforming, plotted as a function of the azimuth-angle separation between transmitters.

tive probabilities of 0.1% to 10%. A SINR of 25-50 dB was measured in urban and rural line-of-sight and non-line-of-sight peer-to-peer scenarios. In multipath channels, these performance levels were achieved even when there was very little separation between the transmitters in azimuth angle, as seen from the receiver (a theodolite on a surveyor's tripod was placed at the receiver location, prior to the measurements, and was used to determine the transmitter locations), and when there was less than 2° difference in the orientations of the two transmitting antennas. For the experiments in which the receiver was hand-carried at walking speeds, the mean SINR improvement in the outdoor suburban line-of-sight peer-to-peer scenario was approximately 37-41 dB, and the mean SINR after beamforming was 21-27 dB in the suburban, mostly non-line-of-sight microcell scenario. The lower SINR in the microcell scenario was partly due to the low SNR, caused by attenuation of the signal over the longer propagation path. In the multipath channels measured, a dual- or multi-polarized antenna array generally provided no more than a 3 dB advantage over a co-polarized array, indicating that in these channels, polarization flexibility can be helpful but is not critical.

6. Conclusions

The value of spatial diversity in base-station antennas has long been recognized. Recent results show that polarization and angle diversity offer similar improvements. Experiments have shown that base-station diversity gains of 5-11 dB at the 1% probability (99% reliability) level are possible with two-branch diversity. Gains of 8-11 dB were observed using spatial diversity; polarization diversity yielded 6-10 dB diversity gain; and angle diversity provided 5-9 dB gain. Polarization and angle diversity have the advantage that the antenna systems are relatively compact. In a cellular system, these diversity gains translate into improved reliability, longer handset talk time, and/or increased range. The effectiveness of spatial, polarization, and pattern diversity for handsets using multiple antenna elements has also been demonstrated.

Adaptive beamforming has been considered for base stations and, more recently, for handsets. Experiments reported here for smart handheld terminals demonstrated over 20 dB of interference rejection with single- and multi-polarized arrays. In many cases, the performance measured in multipath channels was better than the previously-reported simulated performance of comparable arrays in free space. Differences in the angular distribution and the phases of multipath signals allow an adaptive receiving array to distinguish between two transmitters, even if the azimuth angles (as seen from the receiver) and polarization angles of the transmitters are identical. Adaptive beamforming can improve reliability, range, talk time, and capacity in both peer-to-peer and cellular systems.

Smart antennas can improve system performance, and will find increasing use. Applications have been almost exclusively for receiving situations, but smart transmitting antennas will also be used in the future.

7. Acknowledgements

Support of this research from DARPA, Texas Instruments, Metawave, GTE, Verizon, and EMS Wireless is gratefully acknowledged.

8. References

1. R. G. Vaughan, "On Optimum Combining at the Mobile," *IEEE Transactions on Vehicular Technology*, **VT-37**, 4, November 1988, pp. 181-188.

2. K.-J. Lian, "Adaptive Antenna Arrays for Satellite Personal Communication Systems," Master's Thesis, Virginia Tech, January, 1997.

3. C. Braun, M. Nilsson, and R. D. Murch, "Measurement of the Interference Rejection Capability of Smart Antennas on Mobile Telephones," IEEE Vehicular Technology Conference, 1999.

4. R. T. Compton, Jr., "On the Performance of a Polarization Sensitive Adaptive Array," *IEEE Transactions on Antennas and Propagation*, **AP-29**, 5, September 1981, pp. 718-725.

5. R. T. Compton, Jr., "The Tripole Antenna: An Adaptive Array with Full Polarization Flexibility," *IEEE Transactions on Antennas and Propagation*, **AP-29**, 6, November 1981, pp. 944-952.

6. R. T. Compton, Jr., "The Performance of a Tripole Adaptive Array Against Cross-Polarized Jamming," *IEEE Transactions on Antennas and Propagation*, **AP-31**, 4, July, 1983, pp. 682-685.

7. L. B. Preiser, "Polarization Diversity of the General Nonuniformly Spaced Adaptive Array," IEEE International Symposium on Antennas and Propagation *Digest*, 1988, pp. 553-556.

8. I. Kaptsis and K. G. Balmain, "Base Station Multi-polarized Adaptive Antenna for Mobile Radio," International Conference on Universal Personal Communications, 1994, pp. 230-235.

9. B. Vaidyanathan, M. D. Srinath, and G. D. Mandyam, "Dual Polarized Smart Antenna Beams," 46th IEEE Vehicular Technology Conference, 1996, pp. 1675-1679.

10. W. C. Jakes, *Microwave Mobile Communications*, AT&T, 1974 (reprinted by IEEE Press, Piscataway, NJ).

11. Kai Dietze, Carl Dietrich, and Warren Stutzman, "Vector Multipath Propagation Simulator (VMPS)," draft report, Virginia Tech Antenna Group, April 7, 1999.

12. C. B. Dietrich, Jr. and W. L. Stutzman, "Smart Antennas Enhance Cellular/PCS Performance, Part I," *Microwaves & RF*, April 1997, pp. 76-86.

13. C. B. Dietrich, Jr. and W. L. Stutzman, "Smart Antennas Enhance Cellular/PCS Performance, Part II," *Microwaves & RF*, May 1997, pp. 164-168.

14. J. Butler and R. Lowe, "Beam-Forming Matrix Simplifies Design of Electronically Scanned Antennas," *Electronic Design*, April 12, 1961, pp. 170-173.

15. A. W. Rudge et al. (ed.), *The Handbook of Antenna Design, Volume 2*, London, Peter Peregrinus, 1983, pp. 314-316.

16. J. Blass, "Multidirectional Antenna: A New Approach to Stacked Beams," *IRE International Conference Record*, **8** (Part 1), 1960.

17. S. Mano et al., "Application of Planar Multibeam array Antennas to Diversity Reception," *Electronics and Communications in Japan, Part I*, **79**, 11, 1996, pp. 104-112.

18. J. Litva and T. K.-Y. Lo, *Digital Beamforming in Wireless Communications*, Norwood, MA, Artech House, 1996.

19. P. W. Howells, *Intermediate Frequency Sidelobe canceler*, US Patent 3202990, May 1959.

20. S. Applebaum, "Adaptive arrays," Technical Report SPL TR-66-001, Syracuse University Research Corporation, 1965.

21. D. N. Goddard, "Self-Recovering Equalization and Carrier Tracking in a Two-Dimensional Data Communication System," *IEEE Transactions on Communications*, **COM-28**, 1980, pp. 1867-1875.

22. J. R. Treichler and B. Agee, "A New Approach to Multipath Correction of Constant Modulus Signals," *IEEE Transactions on Acoustics, Speech, and Signal Processing*, **ASSP-31**, April 1983, pp. 459-472.

23. B. Agee, "Blind Separation and Capture of Communication Signals Using a Multitarget Constant Modulus Beamformer," *Proceedings of the IEEE Military Communications Conference*, 1989, pp. 340-346.

24. T. Biedka, personal communication, 1997.

25. B. S. Collins, "Polarization Diversity Antennas for Compact Base Stations," *Microwave Journal*, January 2000, pp. 76-88.

26. C Beckman and U. Wahlberg, "Antenna Systems for Polarization Diversity," *Microwave Journal*, May 1997, pp. 330-334.

27. F. Lotse, J-E. Berg, U. Forssen, and P. Idahl, "Base Station Polarization Diversity Reception in Macrocellular Systems at 1800 MHz," *IEEE 46th Vehicular Technology Conference Proceedings, Volume 3*, April 28-May 1, 1996, pp. 1643-1646.

28. J. J. A. Lempiainen and J. K. Laiho-Steffens, "The Performance of Polarization Diversity Schemes at a Base Station in Small/Micro Cells at 1800 MHz," *IEEE Transactions on Vehicular Technology*, **VT-47**, 3, August 1998, pp. 1087-1092.

29. J. J. A. Lempiainen and J. K. Laiho-Steffens, "The Performance of Polarization Diversity Schemes at a Base Station in Small/Micro Cells at 1800 MHz," *IEEE Transactions on Vehicular Technology*, **VT-47**, 3, August 1998, pp. 1087-1092.

30. "Polarization Diversity," EMS Wireless.

31. "Operational Field Tests for DualPol™ Cellular Antenna," EMS Wireless, October 12, 1995.

32. M. J. Feuerstein, "Unlocking the Capacity You Paid For," CDMA Solutions Seminar Series, Seminar One, Metawave, available at http://www.metawave.com/Resources/default.htm .

33. P. L. Perini, C. L. Holloway, "Angle and Space Diversity Comparisons in Different Mobile Radio Environments," *IEEE Transactions on Antennas and Propagation*, **AP-46**, June 1998, pp. 764-775.

34. W. C. Y. Lee, *Mobile Communications Engineering, Second Edition*, New York, McGraw-Hill, 1998, pp. 203-205.

35. W. Y. C. Lee, "Estimate of Local Average Power of a Mobile Radio Signal," *IEEE Transactions on Vehicular Technology*, **VT-34**, February 1985, pp. 22-27.